Support information

Nanocavity-in-Multiple Nanogap Plasmonic Coupling Effects from Vertically Sandwich-like Au@Al_2O_3@Au Arrays for Surface–Enhanced Raman Scattering

Chen Yang,[a] Ying Chen,[a] Dan Liu,[a] Cheng Chen,[a] Jiemin Wang,[a] Ye Fan,[a] Shaoming Huang,[b] and Weiwei Lei*[a]*

[a]Institute for Frontier Materials, Deakin University, Locked Bag 2000, Geelong, Victoria 3220, Australia.

[b]Nanomaterials & Chemistry Key Laboratory, Wenzhou University, Wenzhou, P. R. China.

* E-mail of corresponding authors: ian.chen@deakin.edu.au ; weiwei.lei@deakin.edu.au

1. Chemical component analysis

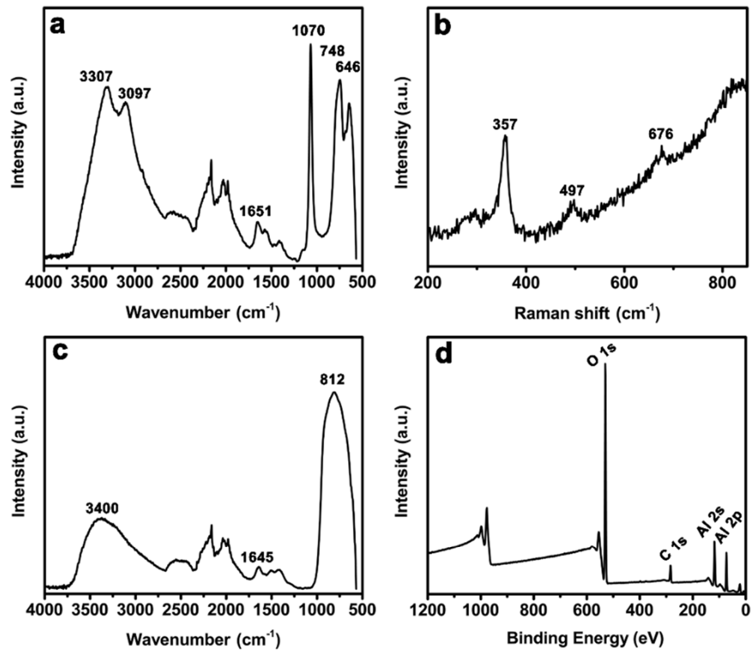

Figure S-1. (a) FT-IR (ATR) spectroscopy and (b) Raman spectra of boehnmite NSs; (c) FT-IR (ATR) spectroscopy and (d) XPS analysis of Al_2O_3 NSs.

Figure S1a illustrated that the characteristic peaks of boehmite NSs in FT-IR (ATR) spectroscopy were located at 3307, 3097, 1651, 1070, 748 and 646 cm^{-1}.[1-3] The peaks at 3307 and 1652 cm^{-1} belonged to the stretching vibration of -OH group and the bending mode in the absorbed water, respectively. The peak at 3097 cm^{-1} discharged from the symmetric stretching vibration of AlO-H. The intense peak at 1070 cm^{-1} ascribed to the bending vibration mode of Al-O-H and bands at 748 and 646 cm^{-1} consisted with the vibration mode of AlO_6. The Raman spectra in Figure S1b further proved the existence of boehmite NSs including the bands at 357, 497 and 676 cm^{-1}.[4]

As showed in Figure S1c, the peaks at 3402, 1645 and 812 cm^{-1} were identified after the RTA process. The peaks at 3402 and 1645 cm^{-1} were from -OH groups of the adsorbed water, while the peak at 812 cm^{-1} were classified into AlO_6.[5] Compared with Figure S1a, it found that the strong peak of 3097 cm^{-1} (the symmetric stretching vibration of AlO-H) and 1070 cm^{-1} (the bending vibration mode of Al-O-H in boehmite) disappeared obviously. Therefore, it demonstrated that the dehydration reaction of boehmite NSs occurred during the RTA process. In addition, by the XPS analysis of Al_2O_3 NSs in Figure S1d, two peaks located at 74.1 eV and 118.9 eV were assigned to Al 2p and Al 2s, respectively. The peak of 531 eV was consistent with O 1s in Al_2O_3 NSs, while 284.8 eV was from C 2s.[6-7] The atomic ratio of Al:O was closely around 2:3. Thus, the XPS tests further confirmed the chemical components of Al_2O_3 NSs. According to the analysis above, we suggested that the formation of Al_2O_3 NSs could be explained as following steps: firstly, Al reacted with H_2O at 120 ℃ to synthesize boehmite NSs on the surface of Al foil; secondly, the large scale of vertical morphology might be due to physically attack of dihydrogen and air bubbles between the interface of H_2O/DMF and Al foil; finally, boehmite NSs dehydrated into generate Al_2O_3 NSs after RTA process.[8-9]

2. Morphologies of Al_2O_3 NSs and sandwich-like Au@Al_2O_3@Au hybrids

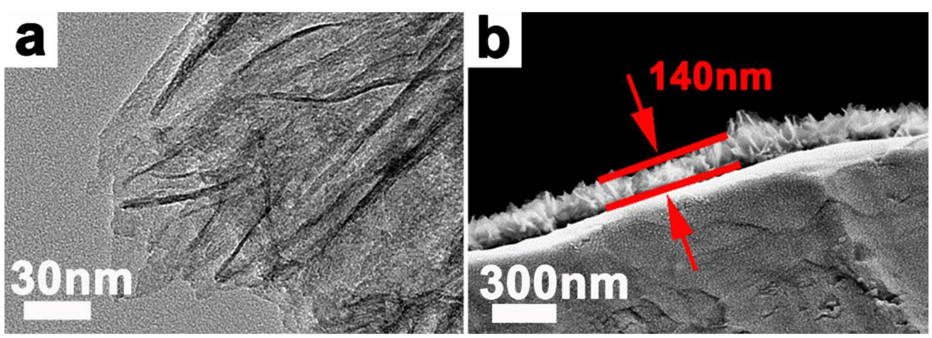

Figure S-2. (a) TEM image of Al_2O_3 NSs and (b) side-view SEM image of vertical Al_2O_3 NSs arrays

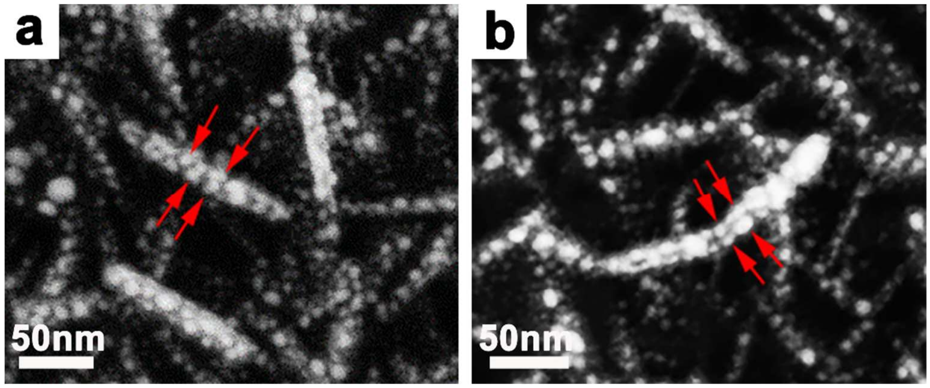

Figure S-3. (a) and (b) Higher magnification SEM images of sandwich-like Au@ Al_2O_3@Au hybrid nanosheets.

3. AFM test of Al_2O_3 NSs and contact angle performance of PSHNs substrates

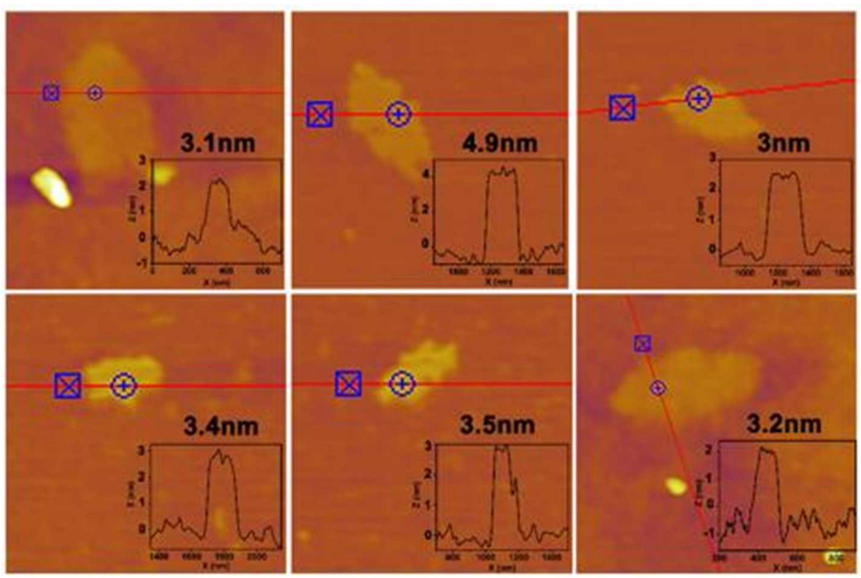

Figure S-4. AFM images of Al_2O_3 NSs on Si substrate.

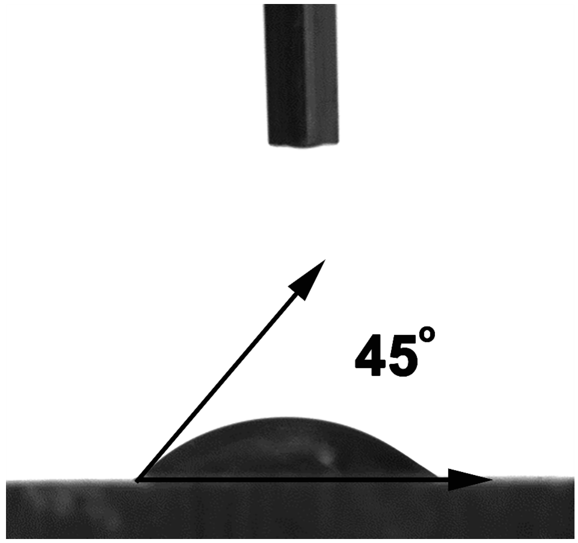

Figure S-5. Contact angle test of 2DT-PSHNs substrate.

4. Analysis of Raman signals

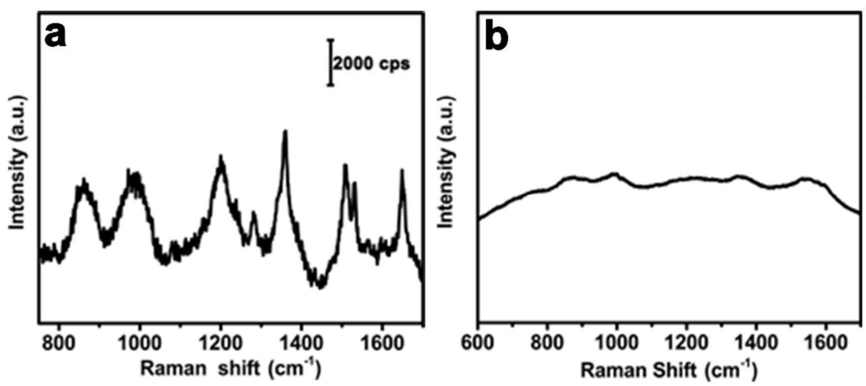

Figure S-6. Raman spectroscopy: (a) original spectral line from Al foil as the non-enhanced substrate; (b) as-used and washed 2DT-PSHNs substrate.

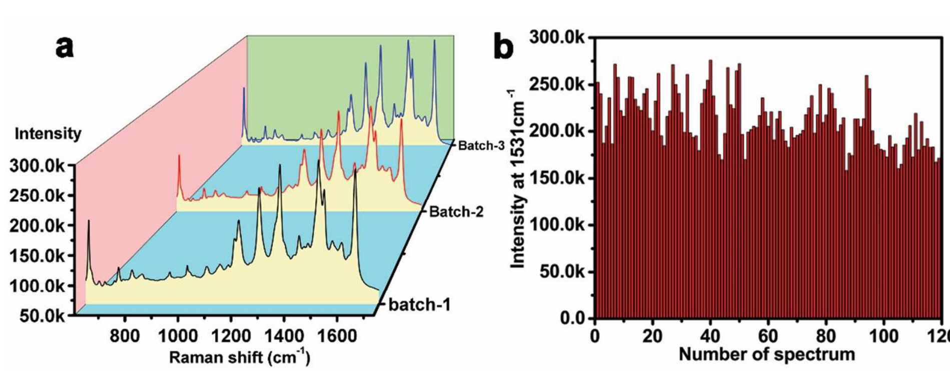

Figure S-7. (a) batch-to-batch and (b) point-to-point SERS reproducibility of 2DT-PSHNs substrates.

Table S-1. Estimation of Raman Enhanced Factors of 2.14 $\times 10^{-16}$M and 10^{-18}M Rh B solution on 1DT-, 2DT- and 3DT-PSHNs substrates.

Sample (3D PSHNs substrates)	Raman shift (996~1000 cm^{-1})	Raman shift (1527~1532 cm^{-1})
1DT-EF_{-16M}	$0.16*10^{10}$	$0.22*10^{10}$
2DT-EF_{-16M}	$1.47*10^{10}$	$2.98*10^{10}$
3DT-EF_{-16M}	$0.62*10^{10}$	$0.49*10^{10}$
1DT-EF_{-18M}	none	$0.20*10^{12}$
2DT- EF_{-18M}	$0.36*10^{12}$	$1.27*10^{12}$
2DT-C2-EF_{-18M}	$0.43*10^{12}$	$1.09*10^{12}$
2DT-C3-EF_{-18M}	$0.71*10^{12}$	$1.30*10^{12}$
2DT-C4-EF_{-18M}	$0.90*10^{12}$	$0.80*10^{12}$
2DT-C5-EF_{-18M}	$0.36*10^{12}$	$1.20*10^{12}$
3DT-EF_{-18M}	$0.46*10^{12}$	none

References

(1) Shi, Z. B.; Jiao, W. Q.; Chen, L.; Wu, P.; Wang, Y. M.; He, M. Y., Clean Synthesis of Hierarchically Structured Boehmite and Gamma-Alumina with a Flower-Like Morphology. *Micropor. Mesopor. Mat.* **2016,** *224*, 253-261.

(2) Cai, Y.; Huang, H. H.; Wang, L.; Zhang, X. J.; Yuan, Y. W.; Li, R.; Wan, H.; Guan, G. F., Facile Synthesis of Pure Phase Gamma-AlOOH and Gamma-Al2O3 Nanofibers in a Recoverable Ionic Liquid via a Low Temperature Route. *RSC Adv.* **2015,** *5* (127), 104884-104890.

(3) Yang, J. X.; Ma, J. J.; Huang, Y. W., Hydrothermal Synthesis of Monodisperse Leaf-Like Boehmite Nanosheets: Transformation from Irregular to Regular Morphology. *Frontier of Nanoscience and Technology* **2011,** *694*, 28-32.

(4) Wang, Z. J.; Tian, Y.; Fan, H. S.; Gong, J. H.; Yang, S. G.; Ma, J. H.; Xu, J., Facile Seed-Assisted Hydrothermal Fabrication of Gamma-AlOOH Nanoflake Films with Superhydrophobicity. *New J Chem.* **2014,** *38* (3), 1321-1327.

(5) Liu, S. L.; Chen, C. Y.; Liu, Q. P.; Zhuo, Y. W.; Yuan, D.; Dai, Z. H.; Bao, J. C., Two-Dimensional Porous Gamma-AlOOH and Gamma-Al_2O_3 Nanosheets: Hydrothermal Synthesis, Formation Mechanism and Catalytic Performance. *RSC Adv.* **2015,** *5* (88), 71728-71734.

(6) Iatsunskyi, I.; Kempiński, M.; Jancelewicz, M.; Załęski, K.; Jurga, S.; Smyntyna, V., Structural and XPS Characterization of ALD Al_2O_3 Coated Porous Silicon. *Vacuum* **2015,** *113*, 52-58.

(7) Jankovský, O.; Šimek, P.; Sedmidubský, D.; Huber, Š.; Pumera, M.; Sofer, Z., Towards Highly Electrically Conductive and Thermally Insulating Graphene Nanocomposites: Al_2O_3–Graphene. *RSC Adv.* **2013,** *4* (15), 7418-7424.

(8). Yamazoe, S.; Naya, M.; Shiota, M.; Morikawa, T.; Kubo, A.; Tani, T.; Hishiki, T.; Horiuchi, T.; Suematsu, M.; Kajimura, M., Large-Area Surface-Enhanced Raman Spectroscopy Imaging of Brain Ischemia by Gold Nanoparticles Grown on Random Nanoarrays of Transparent Boehmite. *ACS Nano* **2014,** *8* (6), 5622-5632.

(9). Peng, S.; Yang, X.; Tian, D.; Deng, W., Chemically Stable and Mechanically Durable Superamphiphobic Aluminum Surface with a Micro/Nanoscale Binary Structure. *ACS Appl. Mater. Inter.* **2014,** *6* (17), 15188-15197.